Title: Vitronectin acts as a key regulator of adhesion and migration in umbilical cord-derived MSCs under different stress conditions

Ankita Sen and Malancha Ta.

Indian Institute of Science Education and Research, Kolkata (IISER Kolkata), India.

Ankita Sen, Email: as17rs015@iiserkol.ac.in
Malancha Ta, Email: malancha.ta@iiserkol.ac.in

Abstract:

Mesenchymal stem cell (MSC)-based cellular therapy gets compromised as adverse microenvironmental conditions like nutrient deprivation, ischemia, hypoxia affect migration and engraftment, in addition to viability, of MSCs at the target site post transplantation. To improve the treatment efficacy, it is critical to identify factors involved in regulating migration and adhesion of MSCs under such microenvironmental stress conditions. In our study, we observed that Wharton's jelly-MSCs (WJ-MSCs) exhibited increase in cell spread area and adhesion with reduction in cellular migration under serum starvation. The changes in adhesion and migration characteristics were accompanied by extensive stress fibre formation and altered ECM gene expression with notable induction in vitronectin (VTN) expression and reduction in MMP-1 expression. Molecular and phenotypic correlative studies advocated the possible role of VTN and not MMP-1, in regulating adhesion and migration of WJ-MSCs. NF-κβ was found to be the positive regulator of VTN expression while ERK pathway regulated it negatively. Further investigation with inhibition of these signalling pathways or VTN knockdown studies under serum starvation established the correlation between increase in VTN expression and increased cellular adhesion with corresponding reduction in migration. VTN knockdown under serum starvation also led to reduction in actin stress fibre along with reversal in expression of several ECM genes. Additionally, VTN induction being absent in hypoxia-treated WJ-MSCs, the hypoxic cells showed no significant change in the adhesion and migration properties. However, when VTN expression was induced under hypoxia by ERK pathway inhibition, similar increase in cell spread area and adhesion was observed. Our study thus highlights VTN as a factor which is induced under serum starvation stress and possibly affects the adhesion and migration properties of WJ-MSCs.

Introduction

Mesenchymal stem cells (MSCs), being hypoimmunogenic, immunomodulatory and reparative in nature, have huge potential for clinical applications as a therapeutic candidate and personalised medicine for treatment of several inflammation-mediated and tissue-injury related diseases [1]. The capability of MSCs to migrate and engraft at the site of injury followed by a balanced secretion of immunomodulatory and regenerative factors in response to the diseased microenvironment makes them a powerful candidate for cell-based therapy [2]. However, MSCs are unable to execute their full beneficial effect as the cells which are being expanded and prepared in favourable *in-vitro* culture conditions for clinical use, are not equipped to withstand the harsh in-vivo microenvironment prevalent at the recipient site due to inflammation or injury [3]. The site of inflammation is commonly marked by hostile microenvironmental conditions like ischemia, oxygen and nutrient deprivation, and

presence of host-derived pro-inflammatory molecules, which could be detrimental to the viability and functionality of MSCs. The efficacy of MSC based cell therapy hence gets compromised as MSCs, post transplantation, exhibit low migration rate and poor tissue engraftment at the site of injury and additionally, undergo significant loss in cell viability [4]. Migration, homing and adhesion are some of the key inherent properties of MSCs which play crucial role in strengthening their viability and functionality [5]. Thus dissecting and understanding the basic regulation mechanisms underlying adhesion and migration of MSCs under stress conditions would help to overcome the current challenges and lead to better performing MSC based therapeutics.

MSCs have been isolated from various adult as well as young tissue sources like bone marrow, adipose tissue, amniotic fluid, umbilical cord etc. via different methods of isolation, such as, enzymatic digestion, explant culture method etc. Depending on the tissue source or the method of isolation and culture, the therapeutic potential and functionality of MSCs may vary [6]. In fact, MSCs from different tissues, while exhibiting certain common basic characteristics, show some innate differences too. MSCs isolated from Wharton's jelly (WJ), which is the perivascular region of umbilical cord, have been shown to possess better immuno-modulatory and regenerative properties along with higher proliferation capability as compared to many adult sources [7].

As MSCs are widely used for cell-based therapy towards ischemic stroke, myocardial ischemic injury and other associated diseases which are marked by nutrient and oxygen deprived micro-environment, identifying the mode of regulation of cell adhesion and migration along with the underlying factors under these stress conditions becomes important for improving the efficacy of treatment. Extra-cellular matrix (ECM) proteins namely fibronectin, vitronectin (VTN) and collagen 1 act as motogenic factors both in soluble and insoluble forms and are known to play significant roles in recruitment of MSCs at the site injury for tissue repair and regeneration [8].

In our previous studies, we had shown that exposure of WJ-MSCs to ischemia-like condition and serum starvation *in-vitro* led to reduction in wound closure rate indicating impaired cell migration and an ECM associated glycoprotein, VTN, also known as serum spreading factor, showed up-regulation [9]. In fact, as some other groups reported in HEK239 cells, VTN regulated morphology and migration of cells via uPAR-matrix interaction [10]. VTN, also known for its adhesive role in tumor micro-environment, promoted tumor metastasis and regulated cell growth in neuroblastoma cells via cell- matrix interaction [11]. It was also demonstrated to interact with both integrin and uPAR via RGD and SMB domains, respectively, which increased the cell attachment by promoting focal adhesion (FA) component rearrangement at the FA sites [12].

Cell adhesion and cell migration usually display a biphasic relationship, whereby cell migration is maximum when cell-matrix adhesion is neither too high nor too low [13]. Here, we observed that cell adhesion and migration of WJ-MSCs were altered on exposure to serum starvation condition *in-vitro* wherein cell adhesion increased with a corresponding decrease in cell migration. In parallel, an increase in VTN expression was noted in the serum-starved WJ-MSCs. By independently inhibiting ERK and NF-kB signalling pathways, regulation of VTN expression was established by these two pathways. In addition, changes in morphology, adhesion and migration of WJ-MSCs under serum starved condition strongly correlated with induced VTN expression. VTN silencing studies further confirmed its role in impacting altered morphology, adhesion and migration of serum-starved WJ-MSCs. VTN knockdown also led to reversal in expression of ECM genes like collagens along with reduction in accumulated actin stress fibres observed under serum starved condition.

Physiological condition of ischemia is often marked by hypoxia. In the meantime, MSCs have been shown to reside in low oxygen tension in the natural in vivo niche. Next, on subjecting WJ-MSCs to hypoxia condition *in-vitro*, interestingly, we noted that there was no change in migration rate or pattern of cells under hypoxia as compared to control WJ-MSCs, which corresponded well with the fact that there was no notable difference in the expression level of VTN either. But, on inhibiting ERK

pathway, the negative regulator of VTN expression, there was a marked increase in cell spread area and cellular adhesion corresponding to the induction in VTN expression under hypoxia.

Thus, our study establishes that VTN plays an important role in regulating the migration and adhesion of WJ-MSC under different stress conditions. This study thus offers new perspectives to modulate MSC migration and adhesion under stress conditions, which could help improve their efficacy following transplantation.

Material and methods:

Cell culture:

Human umbilical cords were collected after full term births (vaginal or cesarean delivery) with informed consent of the donor following the guidelines laid down by Institutional Ethics Committee (IEC) and Institutional Committee for Stem Cell Research and Therapy (IC-SCRT) at IISER, Kolkata, India. WJ-MSCs were isolated from the perivascular region of the umbilical cord termed as Wharton's jelly by explant culture method as described previously [14]. All experiments were performed between passages 4 to 6 where cells were dissociated using TrypLE express (Life technologies), a gentle animal origin-free recombinant enzyme and seeded at a cell density of 5000 cells/cm^2.

WJ-MSCs were initially cultured in complete medium comprising of KnockOut DMEM (Dulbecco's modified Eagle's medium) supplemented with 10% FBS, 2mM Glutamine and 1X PenStrep (all from Life technologies). For serum starvation stress, after 24 hours, cells were serum starved for the next 48 hours by replacing the medium with KnockOut DMEM medium supplemented with 2mM Glutamine and 1X PenStrep but no serum. For hypoxia treatment, cells were exposed to 2% oxygen for 48 hours and grown in complete medium comprising of KnockOut DMEM supplemented with 10% FBS, 2mM Glutamine and 1X PenStrep. Corresponding to the *in-vitro* serum starvation stress and hypoxia condition, the control cells were grown in complete medium for a total duration of 72 hours, in parallel. For different signalling pathway inhibition studies, cells were treated with specific small molecule inhibitors and their respective vehicle controls under serum starved condition or hypoxia for a period of 48 hours. ERK pathway inhibitor, FR-180204 and NF-kB pathway inhibitor, BAY 11-7082 were added at an optimized concentration of 30uM and 4uM respectively (both from Sigma-Aldrich).

siRNA transfection for knockdown studies:

For siRNA mediated knockdown studies, WJ-MSCs were grown for 24-36 hours till they reached around 50-60% confluency. Transfection was performed using Lipofectamine 3000 in Opti-MEM I (both from Life Technologies) medium as per manufacturer's protocol. For VTN and NF-κβ knockdown studies, endonuclease- treated siRNA pool (esiRNA) generated against VTN and p65 (all from Sigma-Aldrich) were used while for experimental control, mission universal negative control siRNA was used and all at a concentration of 30nM each. After 18-20 hours post transfection, WJ-MSCs were exposed to serum starvation for the next 36-48 hours and harvested as per the experimental requirement.

Cell spread area calculation:

For quantification of alteration in cell morphology, cell spread area of WJ-MSCs which were exposed to different experimental conditions was measured using ImageJ (NIH) software. Phase contrast imaging of WJ-MSCs was performed using Nikon Eclipse TS100 inverted microscope (Nikon) at 10X magnification. Cell spread area was calculated for 50 cells each from 3 independent biological samples and the data was plotted by fitting the data into Gaussian distribution using GraphPad Prism 8 software (GraphPad) to represent the cell spread area distribution across the population.

De-adhesion dynamics:

To study the alteration in adhesion property of WJ-MSCs under serum starved condition, cell de-adhesion dynamics was quantified by performing live cell time lapse imaging following treatment with 0.5mM EDTA (Sigma-Aldrich) . For the experiment, live cells were treated with 0.5mM of EDTA and live cell imaging was performed using Olympus IX81 (Olympus) microscope to capture de-adhesion of the cells from the surface. Change in cell spread area across time was calculated and the normalized cell spread area was plotted against time. The data was fitted in Boltzmann's equation in GraphPad Prism 8 software (GraphPad), from which two time constants were obtained which gave the quantitative measure of adhesion property of cells.

Wound healing assay:

To understand the effect of serum starvation on migration of WJ-MSCs, wound healing assay was performed. WJ-MSCs were seeded at a cell density of 6000 cells/cm^2 and next, control or treated cells were scraped using a sterile micro-tip to create a uniform wound on the confluent monolayer of cells. Phase contrast imaging was performed at an interval of 2 hours till wound closure using Olympus IX81 inverted microscope (Olympus) at 10X magnification and the micromanager software. The wound closure rate was quantified by measuring the change in the width of the wound across time using the ImageJ (NIH) software.

Time lapse imaging:

To further evaluate the migration pattern, directionality and migration rate of WJ-MSCs under serum starved condition, cells were plated at a cell density of 4000 cells/cm^2 in glass bottom dishes (SPL Lifesciences) and time lapse imaging was performed for a duration of 3 hours by capturing images at a frequency of 1 frame/ min in confocal microscope LSM 710 (Axio Observer Z1, Carl Zeiss) equipped with an environmental chamber set at 37°C with 5% CO_2. At least 50 cells per condition from three independent biological samples were analysed. The cell XY co-ordinates were obtained at each time point using ImageJ software (NIH) following which cell directionality, trajectory pattern and mean square displacement was quantified using DiPer software [15] and the cell migration rate was calculated using ZEN software (Zeiss).

RNA isolation and cDNA synthesis:

Total RNA was isolated using Trizol (Sigma-Aldrich) and the RNA yield was quantified using Nanodrop 2000 spectrophotometer (Thermo Scientific). cDNA synthesis was done using Verso cDNA synthesis kit (Thermo Scientific).

Quantitative reverse transcription polymerase chain reaction:

To quantify the mRNA expression of relevant genes, qRT-PCR reactions were done with PowerUp SYBR™ Green Master mix (Applied Biosystems) using ABI Biosystems 7500HT instrument (Applied Biosystems). The fold change in mRNA expression was quantified by $2^{-\Delta\Delta CT}$ method using compatible Applied Biosystems software. Validation of single, specific PCR products was done via

melting curve analysis. *GAPDH* was considered as the endogenous control gene. The primer sequences and amplicon sizes are listed in supplementary table.

Western Blotting:

For quantification of protein expressed by WJ-MSCs under serum starvation, whole cell lysates were prepared using RIPA lysis buffer along with protease inhibitor cocktail (all from SantaCruz Biotechnology). For quantification of MMP-1 protein expression which is a secretory protein, condition medium was collected and lyophilized to concentrate the sample. Protein concentration in both whole cell lysate and concentrated condition medium was quantified by Bradford assay. Polyacrylamide gel electrophoresis and western blotting were performed as per standard protocol. Primary and secondary antibodies used were anti-p65 (Santa Cruz Biotechnology), anti-VTN (Santa Cruz Biotechnology), anti-MMP-1 (R&D Systems), anti-GAPDH (Santa Cruz Biotechnology) and HRP-linked anti-mouse IgG (Cell Signalling Technology).

Immunofluorescence staining:

To study the cytoskeleton arrangements in WJ-MSCs on exposure to different treatments, immunofluorescence phalloidin staining was performed as per standard protocol. The cells were grown on glass coverslips and exposed to specific treatment conditions as per the experiment and were fixed with 4% para-formaldehyde for 20 mins at room temperature. The fixed cells were permeabilized using 0.1% Triton X-100 (Sigma-Aldrich) for 10 mins and actin cytoskeleton was stained using Alexa Fluor™ 488 Phalloidin (Invitrogen) at room temperature for 1 hr. DAPI (Sigma-Aldrich) was used to stain the nucleus and then the coverslips were mounted on glass slides using VECTASHIELD anti-fade mounting medium. The images were captured using ZEN software (Zeiss) at 40x magnification in Zeiss Apotome module microscope.

Statistical Analysis:

All data are presented as mean ± standard error of the mean (SEM) from at least 3 independent biological samples. Data analysis and graphical representations were performed using GraphPad Prism 5/ 8 software (GraphPad). Statistical comparisons were assessed using the two-tailed Student t-test or one-way ANOVA. Significance was accepted at $p \leq 0.05$.

Results:

Serum starvation impairs the migration ability of the WJ-MSCs

As reported previously [16], exposure to serum starved condition resulted in flattened morphology with significant increase in cell spread area (data not shown) and cellular adhesion in WJ-MSCs (Fig. 1A, B). For the de-adhesion assay, a minor modification was introduced here where MSCs were treated with warm EDTA only. A slower de-adhesion was reflected by the right shift of the sigmoidal curve (Fig. 1A) along with increase in $\tau 1$ and $\tau 2$ values from 15.48±0.93s to 79.5±5.85s and 7.38±0.56 to 30.52±1.67, respectively. In addition to these phenotypic changes, here we sought to investigate the effect of serum starvation stress on cell migration of WJ-MSCs.

First, cell migration was assayed via *in-vitro* scratch-induced wound healing assay (Fig. 1C). Cell migration rate, assessed during wound closure, indicated that serum-starved WJ-MSCs exhibited slower wound closure rate (27.6±3.5 um/hr) compared to control condition (49.9±6.8 um/hr) (Fig. 1D; $p < 0.05$).

To analyse the above more thoroughly, we next investigated the impact of serum starvation on the migration pattern of WJ-MSCs and live cell time lapse imaging was performed (Fig. 1E). Cell migration was quantified in terms of single cell migration rate, single cell trajectory pattern, directionality ratio and mean square displacement using ZEN and DiPer software [15] (Fig. 1F, G-I). Both single cell migration rate and mean square displacement data indicated that the cell migration decreased significantly on exposure to serum starvation compared to the control condition. Corresponding to the change in migration rate, the single cell trajectory pattern showed lower spread area indicating impaired migration of serum-starved WJ-MSCs along with loss of directionality as also suggested by the directionality ratio plot (Fig. H).

Reciprocal expression and regulation of VTN and MMP-1 in WJ-MSCs under serum starved condition

Next, we investigated the expression and regulation of both VTN and MMP-1 under serum starved condition in co-relation with the phenotypic changes observed. In our previous studies [16,17], we had observed that expression of VTN, an ECM component known to be responsible for cell adhesion, was up-regulated under both serum starvation and febrile temperature stress conditions and this was accompanied by increase in cell spread area and cell adhesion. In the present study, under serum starved condition, VTN expression exhibited a strong upregulation while MMP-1 expression went down both at mRNA and protein levels, respectively (Fig. 2A-D). To determine the signalling pathways involved in regulating the expression of *VTN* and *MMP-1* at the mRNA level, WJ-MSCs were treated with different small molecule inhibitors for different signalling pathways. The data highlighted that ERK and NF-kB signalling pathways could be the two possible signalling pathways involved in regulating VTN and MMP-1 expression.

Inhibition of ERK pathway by small molecule inhibitor, FR180204 under serum starved condition further increased the expression of VTN both at mRNA and protein levels compared to only serum starved condition, though not significant, indicating that ERK signalling pathway negatively regulated the expression of VTN (Fig.2A,C). But the expression of MMP-1 with ERK pathway inhibition remained similar to serum starved condition at both mRNA and protein levels (Fig. 2B, D). While NF-kB pathway inhibition by siRNA mediated knockdown of NF-kB subunit, p65 (Fig. 2E) showed that NF-kB signalling pathway regulated VTN expression positively, as NF-kB pathway inhibition reversed the induced expression of VTN under serum starvation condition (Fig. 2F, H)

In parallel, siRNA mediated knockdown of NF-kB pathway resulted in reversal in *MMP-1* gene expression under serum starved condition, though not significant (Fig. 2 G, I). This indicated that NF-kB signalling pathway negatively regulated the MMP-1 expression but ERK pathway inhibition under serum starvation did not cause any further change in its expression at both mRNA and protein levels.

Silencing of ERK and NF-kb pathways led to phenotypic alterations in WJ-MSCs under serum starved condition

To validate whether VTN and MMP-1 could be the possible genes responsible for causing alterations in properties like increase in cell spread area, cell adhesion and decrease in cell migration accompanying serum starvation, we analysed these phenotypic attributes of WJ-MSCs under ERK or NF-kB pathway inhibition.

It was observed that cell spread area, along with cell adhesion exhibited further increase on inhibiting ERK pathway under serum starved condition (Fig. 3A-D; $p < 0.0001$). The cell adherence was quantified in terms of the de-adhesion dynamics of the cell where cell adhesions were severed by EDTA treatment and cellular detachment phenomena was analysed as decrease in cell spread area with respect to time. The further increase in $\tau 1$ and $\tau 2$ values from 59.32±3.7s to 93.69±5.5s and 24.63±1.28s to 38.87±1.96s to respectively on ERK pathway inhibition clearly indicated that WJ-MSCs adhered more strongly on ERK pathway inhibition compared to serum starvation (Fig. 3D).

Also, ERK pathway inhibition under serum starved condition led to stronger decrease in cellular migration compared to serum starved condition. The wound closure rate reduced from 31.54±1.89 µm/hr to 15.12±2.64 µm/hr as observed by *in-vitro* wound healing assays (Fig. 3E, F; $p < 0.05$).

In contrast, NF-kB pathway silencing via p65 knockdown led to reduction in cell spread area and cellular adhesion (Fig. 3G-J). Faster de-adhesion was assessed from left shift of the sigmoidal curve and also, the τ1 and τ2 graphs showed that siRNA mediated knockdown of p65 led to reduction in time constant values from 49.15±2.5s to 16.43±0.97s and 23.2±1.28s to 8.68±0.5s, respectively compared to negative control siRNA treated WJ-MSCs under serum starved condition (Fig. 3J; $p < 0.0001$). Further, the reduced cell migration also got rescued with p65 knockdown under serum starved condition, though not significant, as evident from increase in the wound closure rate shown in the *in-vitro* wound healing assay data (Fig. 3K).

Overall, we observed that increase in VTN expression corresponded to increase in cell spread area and cellular adhesion along with reduction in cellular migration, and vice-versa. And rescue in MMP-1 expression under p65 knockdown condition corresponded to rescue in cell migration. However, with ERK pathway silencing under serum starved condition, though MMP-1 expression did not change significantly, it resulted in further decrease in cell migration.

VTN regulates the morphology, adhesion and migration of WJ-MSCs under serum starved condition

Furthermore, to specifically verify the role of VTN in regulation of altered adhesion and migration of WJ-MSCs under serum starved condition, we analysed the effect of siRNA mediated silencing of VTN on the altered phenotypic attributes under serum starved condition. We observed that siRNA mediated knockdown of VTN (Fig. 4A) led to distinct reversal in cell morphology (Fig. 4B, C; $p < 0.0001$) and cell adhesion (Fig. 4D; $p < 0.0001$) compared to serum starved condition. Knockdown of VTN resulted in decrease in t1 and t2 values from 48.7±2.29s to 14.23±0.97s and 23.05±1.2 to 7.4±0.5s respectively as obtained from the sigmoidal curve of de-adhesion dynamics indicating that VTN played an important role in promoting cellular adhesion under serum starved condition (Fig. 4D). Along with change in cellular morphology, serum starvation also resulted in huge increase in F-actin in the form of stress fibres, which was also reversed with VTN knockdown as indicated by phalloidin staining. Mean intensity quantification of immunofluorescence for phalloidin staining confirmed the same (Fig 4E; $p < 0.0001$) Further, impaired migration of WJ-MSCs under serum starved condition also got rescued post VTN knockdown as evident from improved single cell trajectory pattern and increased directionality ratio plots (Fig. 4G, I). Along with the recovery in migration pattern, single cell migration rate and the mean square displacement of cells also got rescued with VTN knockdown under serum starved condition (Fig. 4H, J).

Interestingly, *MMP-1* expression got strongly up-regulated at mRNA level (Fig. 4K; $p < 0.01$) with VTN knockdown under serum starvation. This indicated that VTN could be involved in regulating the expression of MMP-1, and possibly other ECM genes, as a consequence of which the adhesion and migration parameters got altered under serum starved condition. Collagen is one of the major components of the ECM and there are 28 different types [18]. They play important functional roles in cell adhesion, migration, differentiation, regeneration etc. On investigating, increased expression of several collagen molecules, *COL IA*, *COL 12A*, *COL 11A* under serum starvation condition was noted, which was reversed when VTN was knocked down, as presented in Fig. 4K.

VTN expression corresponded to change in morphology, adhesion and migration of WJ-MSCs under hypoxia condition.

A hypoxic microenvironment is associated with physiological stem cell niche and is known to support and improve survival and migration of MSCs [19]. Thus, to compare against serum starvation stress where the adhesion and migration of WJ-MSCs got adversely affected, we next exposed WJ-MSCs to

a hypoxic milieu of 2% O2 and studied the expression of VTN and analysed the adhesion and migration of WJ-MSCs under hypoxia to further validate the role of VTN. Interestingly, under hypoxia condition, WJ-MSCs attained small spindle shaped morphology (Fig. 5A, B) with reduced adhesion as compared to control condition (Fig. 5D). The cell trajectory pattern and the directionality ratio mostly remained unaltered with slight increase in migration rate under hypoxia condition (Fig. 5E-G). Corresponding to these basic characteristics, VTN expression either slightly reduced or remained unaltered under hypoxia treatment in contrast to serum starvation, while MMP-1 expression was down-regulated as under serum starvation (Fig. 5H, I). Phalloidin staining of hypoxia treated WJ-MSCs did not show any accumulation of actin stress fibres as seen under serum starvation, and the overall mean intensity of phalloidin staining also remained similar between control and hypoxic-WJ-MSCs (Fig. 5J). Thus, the alterations in phenotypic properties of WJ-MSCs witnessed under serum starvation were absent under hypoxia treatment where there is no induction in VTN expression.

Inhibition of the negative regulator, ERK pathway with small molecule inhibitor FR180204, led to induction in VTN expression at both mRNA and protein levels under hypoxia condition (Fig. 5K, L). And corresponding to the increase in VTN expression, the cells obtained flattened morphology with increase in cell spread area (Fig. 5M) and cellular adhesion. The significant increase in $\tau 1$ and $\tau 2$ values with ERK pathway inhibition under hypoxia condition established that induction of VTN was responsible for the change in cellular adhesion (Fig. 5N).

Discussion:

Though MSCs appear as one of the promising resources due to their paracrine, immunomodulatory and regenerative properties along with their homing ability to the inflamed and injured tissue [20], their potential and utility get compromised due to several factors like non-optimal culture conditions or source of MSCs, mode of administration and host microenvironment. Post transplantation, along with survival, efficient migration and engraftment of the MSCs in adequate numbers are the key to effective MSC-based treatment. However, exposure to hostile microenvironment prevalent in the damaged or diseased tissue, hamper these features [21]. Hence, exploring the mechanisms and key factors involved in migration of MSCs under hostile micro-environment becomes critical.

Nutrient starvation is one of the major micro-environment stress conditions involved with injury and inflammation, which could affect retention and functionality of MSCs in vivo. In MSCs, serum deprivation has been reported to reduce cellular proliferation and upregulate gene expression associated with maintenance of stemness, angiogenesis and endothelial differentiation [22]. A previous publication from our group showed that on exposure to serum starvation for 48 hours, WJ-MSCs retained their viability comparable to control conditions [16]. A study based on preconditioning of bone marrow MSCs with hypoxia and serum deprivation for treatment of ischemic perfusion injury showed that migration of MSCs got reduced on exposure to such stress conditions [23]. However, another contrasting report had shown that serum-deprived MSCs secreted anti-apoptotic factors and had 3-fold increased cellular motility compared to control MSCs [24]. Our current study with WJ-MSCs established that exposure to serum starvation for 48 hours led to significant increase in cell spread area along with increase in cellular adhesion. In parallel, serum starvation reduced the migration rate, and affected mean square displacement and directionality ratio of WJ-MSCs.

Adhesion and migration of cells are profoundly regulated by the interaction of the cells with their surrounding microenvironment via the ECM signalling [25]. Direct coupling between the cell and ECM at the integrin based adhesion sites allow the cells to alter their mechanism of migration based on the changes sensed in the surrounding environment [26]. Previous study of our group show that altered adhesion and migration of WJ-MSCs under febrile temperature stress corresponded to changes in expression of ECM genes like collagens, MMPs and VTN [17]. Here we have investigated the possible role and mechanism of action of ECM genes- VTN and MMP-1 in regulation of adhesion and migration of WJ-MSCs under serum starvation stress. VTN is an adhesive multifunctional

glycoprotein, known to promote cell adhesion, migration and matrix degradation by binding to integrins, PAI and uPAR, thereby facilitating tissue repair and regeneration [11], while MMP-1 is a matrix remodelling metalloproteinase which is reported as the positive regulator of migratory capacity of MSCs [27]. In serum-starved WJ-MSCs, we observed that VTN and MMP-1 had an inverse expression pattern, where expression of VTN got upregulated while MMP-1 expression got down-regulated. The observed inverse expression of VTN and MMP-1 corresponded, as expected, to increase in adhesion and reduction in migration of WJ-MSCs on serum starvation.

Cell adhesion and migration are coordinated and regulated phenomena which get impacted by extracellular signals activating different signal transduction pathways via various surface receptors. Integrin mediated activation of ERK signalling was shown to positively regulate migration of MSCs via activation of FAK pathway [28, 29]. A recent report showed that IL-1B induced migration of human umbilical cord derived MSCs (hUCMSCs) was attenuated by inhibition of ERK, JNK and Akt pathways [30]. In our study with serum-starved WJ-MSCs, the NF-kB signalling pathway was found to be a positive regulator of VTN expression while MMP1 was found to be negatively regulated by it. As per expectation, inhibition of NF-kB pathway via the p65 knockdown approach resulted in reduction of cellular adhesion and rescue in impaired migration. In addition, ERK signalling pathway appeared to be a negative regulator of VTN while not affecting MMP1 expression in serum starved WJ-MSCs. Thus, ERK pathway inhibition led to further upregulation of VTN expression while MMP-1 expression remained unchanged. Interestingly this led to further increase in adhesion and reduction in migration, highlighting a primary role of VTN but not MMP-1 in regulating adhesion and migration of WJ-MSCs under serum starvation

The correlation of increase in VTN expression and increased adhesion along with reduced migration was further validated via VTN knockdown studies. Knockdown of VTN led to similar reversal in adhesion and migration pattern as observed with p65 knockdown studies under serum starvation. Thus, increase in VTN expression possibly resulted in stronger adhesion of WJ-MSCs which in turn impaired the migration capacity of WJ-MSCs under serum starvation.

Knockdown of VTN also led to the reduction in the extensive actin stress fibres formed on exposure to serum starvation. Simultaneously, there was reduction in mRNA expression of collagens, known contributors of ECM stiffness, which were upregulated under serum starvation treatment. A previous report on human MSCs documented that the actin cytoskeleton defines the mechanical properties of the cell, where the actin stress fibre being one of the stiffest structures within the cell, is known to regulate the overall cellular stiffness [31]. It has been reported that in the absence of any chemical stimuli, mechanical property of substrate may also influence the migration activity of cells. Study based on migration of smooth muscle cells on different substrate demonstrate that random migration depends on ECM stiffness in a biphasic manner, whereby beyond an optimal stiffness cell migration reduces [32]. Thus, the observed alteration in migration pattern in WJ-MSCs on serum starvation treatment might be due to the remodelling of ECM via VTN activated signalling cascade resulting to increase in stiffness and cellular adhesion.

Previous reports showed that hypoxia treatment improves physiological behaviour of MSCs supporting their growth and migration, which is contrasting to the impact of serum starvation [33]. Thus, to further affirm the role of VTN as the master regulator of the altered physiological attributes of WJ-MSCs, the adhesion and migration pattern of WJ MSCs were evaluated under hypoxia condition, a natural micro-environment condition associated with stem cell niche, where almost no induction in VTN gene expression was observed. WJ-MSCs exposed to hypoxia condition (2% O2) had similar actin cytoskeleton arrangement with adhesion and migration pattern comparable to control condition. Also, it is important to note that *MMP-1* expression was downregulated under hypoxia indicating that it possibly was not the regulatory factor associated with the alterations noted in adhesion and migration in WJ-MSCs under stress. It was also observed that induction of VTN under

hypoxia by ERK pathway inhibition led to increase in cell spread area and adhesion under hypoxia condition.

Thus, throughout the study it was noted that induction of VTN led to increase in cell spread area and adhesion while migration got reduced indicating VTN as the key factor in regulating adhesion and migration of WJ-MSCs under different stress condition.

References

1. Mastrolia I, Foppiani EM, Murgia A, et al. Challenges in Clinical Development of Mesenchymal Stromal/Stem Cells: Concise Review. Stem Cells Transl Med. 2019;8(11):1135-1148. doi:10.1002/sctm.19-0044
2. Wu X, Jiang J, Gu Z, et.al. Mesenchymal stromal cell therapies: immunomodulatory properties and clinical progress. Stem Cell Res Ther. 2020;11(1):345. doi:10.1186/s13287-020-01855-9
3. Pittenger MF, Discher DE, Péault BM,et.al. Mesenchymal stem cell perspective: cell biology to clinical progress. NPJ Regen Med. 2019;4:22. doi:10.1038/s41536-019-0083-6
4. Baldari S, Di Rocco G, Piccoli M, et.al. Challenges and Strategies for Improving the Regenerative Effects of Mesenchymal Stromal Cell-Based Therapies. *Int J Mol Sci*. 2017;18(10):2087. doi:10.3390/ijms18102087
5. Ocansey DKW, Pei B, Yan Y, et al. Improved therapeutics of modified mesenchymal stem cells: an update. J Transl Med. 2020;18(1):42. doi:10.1186/s12967-020-02234-x
6. Levy O, Kuai R, Siren EMJ, et al. Shattering barriers toward clinically meaningful MSC therapies. Sci Adv. 2020;6(30):eaba6884. doi:10.1126/sciadv.aba6884
7. Marino L, Castaldi MA, Rosamilio R, et al. Mesenchymal Stem Cells from the Wharton's Jelly of the Human Umbilical Cord: Biological Properties and Therapeutic Potential. Int J Stem Cells. 2019;12(2):218-226. doi:10.15283/ijsc18034.
8. Thibault MM, Hoemann CD, Buschmann MD. Fibronectin, vitronectin, and collagen I induce chemotaxis and haptotaxis of human and rabbit mesenchymal stem cells in a standardized transmembrane assay. Stem Cells Dev. 2007;16(3):489-502. doi:10.1089/scd.2006.0100
9. Himal I, Goyal U, Ta M. Evaluating Wharton's Jelly-Derived Mesenchymal Stem Cell's Survival, Migration, and Expression of Wound Repair Markers under Conditions of Ischemia-Like Stress. Stem Cells Int. 2017;2017:5259849. doi:10.1155/2017/5259849
10. Madsen CD, Ferraris GM, Andolfo A,et.al. uPAR-induced cell adhesion and migration: vitronectin provides the key. J Cell Biol. 2007;177(5):927-939. doi:10.1083/jcb.200612058
11. Burgos-Panadero R, Noguera I, Cañete A,et.al. Vitronectin as a molecular player of the tumor microenvironment in neuroblastoma. BMC Cancer. 2019;19(1):479. doi:10.1186/s12885-019-5693-2
12. Madsen CD, Sidenius N. The interaction between urokinase receptor and vitronectin in cell adhesion and signalling. Eur J Cell Biol. 2008;87(8-9):617-629. doi:10.1016/j.ejcb.2008.02.003
13. Schwartz MA, Horwitz AR. Integrating adhesion, protrusion, and contraction during cell migration. Cell. 2006;125(7):1223-1225. doi:10.1016/j.cell.2006.06.015
14. Goyal U, Sen A, Ta M. Isolation and Molecular Characterization of Progenitor Cells from Human Umbilical Cord. *Methods Mol Biol*. 2019;2029:1-13. doi:10.1007/978-1-4939-9631-5_1
15. Gorelik R, Gautreau A. Quantitative and unbiased analysis of directional persistence in cell migration. *Nat Protoc*. 2014;9(8):1931-1943. doi:10.1038/nprot.2014.131

16. Goyal U, Ta M. A novel role of vitronectin in promoting survival of mesenchymal stem cells under serum deprivation stress. Stem Cell Res Ther. 2020;11(1):181. doi:10.1186/s13287-020-01682-y
17. Sen A, Ta M. Altered Adhesion and Migration of Human Mesenchymal Stromal Cells under Febrile Temperature Stress Involves NF-κβ Pathway. *Sci Rep*. 2020;10(1):4473. doi:10.1038/s41598-020-61361-z
18. Yue B. Biology of the extracellular matrix: an overview. J Glaucoma. 2014;23(8 Suppl 1):S20-S23. doi:10.1097/IJG.0000000000000108
19. Lambertini E, Penolazzi L, Angelozzi M, et al. Hypoxia Preconditioning of Human MSCs: a Direct Evidence of HIF-1α and Collagen Type XV Correlation. Cell Physiol Biochem. 2018;51(5):2237-2249. doi:10.1159/000495869
20. Zhuang WZ, Lin YH, Su LJ, et al. Mesenchymal stem/stromal cell-based therapy: mechanism, systemic safety and biodistribution for precision clinical applications. J Biomed Sci. 2021;28(1):28. doi:10.1186/s12929-021-00725-7
21. Musiał-Wysocka A, Kot M, Majka M. The Pros and Cons of Mesenchymal Stem Cell-Based Therapies. Cell Transplant. 2019;28(7):801-812. doi:10.1177/0963689719837897
22. Chua KH, Raduan F, Wan Safwani WK, Manzor NF,et.al. Effects of serum reduction and VEGF supplementation on angiogenic potential of human adipose stromal cells in vitro. Cell Prolif. 2013;46(3):300-311. doi:10.1111/cpr.12029
23. Sun X, Fang B, Zhao X,et.al. Preconditioning of mesenchymal stem cells by sevoflurane to improve their therapeutic potential. PLoS One. 2014;9(3):e90667. doi:10.1371/journal.pone.0090667
24. Sanchez CG, Penfornis P, Oskowitz AZ, et al. Activation of autophagy in mesenchymal stem cells provides tumor stromal support. Carcinogenesis. 2011;32(7):964-972. doi:10.1093/carcin/bgr029.
25. Kim SH, Turnbull J, Guimond S. Extracellular matrix and cell signalling: the dynamic cooperation of integrin, proteoglycan and growth factor receptor. J Endocrinol. 2011;209(2):139-151. doi:10.1530/JOE-10-0377
26. Doyle AD, Carvajal N, Jin A,et.al. Local 3D matrix microenvironment regulates cell migration through spatiotemporal dynamics of contractility-dependent adhesions. Nat Commun. 2015;6:8720. doi:10.1038/ncomms9720
27. Ho IA, Chan KY, Ng WH, et.al. Matrix metalloproteinase 1 is necessary for the migration of human bone marrow-derived mesenchymal stem cells toward human glioma. Stem Cells. 2009;27(6):1366-75. doi: 10.1002/stem.50.
28. Shi Y, Xia YY, Wang L,et.al. Neural cell adhesion molecule modulates mesenchymal stromal cell migration via activation of MAPK/ERK signaling. Exp Cell Res. 2012;318(17):2257-67. doi: 10.1016/j.yexcr.2012.05.029.
29. Tang JM, Yuan J, Li Q, et.al. Acetylcholine induces mesenchymal stem cell migration via Ca2+/PKC/ERK1/2 signal pathway. J Cell Biochem;113(8):2704-13. doi: 10.1002/jcb.24148.
30. Chang CH, Lin YL, Tyan YS,et.al. Interleukin-1β-induced matrix metalloproteinase-3 via ERK1/2 pathway to promote mesenchymal stem cell migration. PLoS One. 2021;16(5):e0252163. doi: 10.1371/journal.pone.0252163.
31. Mathieu PS, Loboa EG. Cytoskeletal and focal adhesion influences on mesenchymal stem cell shape, mechanical properties, and differentiation down osteogenic, adipogenic, and chondrogenic pathways. Tissue Eng Part B Rev. 2012;18(6):436-44. doi: 10.1089/ten.TEB.2012.0014.
32. Peyton SR, Putnam AJ. Extracellular matrix rigidity governs smooth muscle cell motility in a biphasic fashion. J Cell Physiol. 2005 ;204(1):198-209. doi: 10.1002/jcp.20274.

33. Antebi B, Rodriguez LA , Walker KP, et al. Short-term physiological hypoxia potentiates the therapeutic function of mesenchymal stem cells. Stem Cell Res Ther. 2018;9(1):265. doi:10.1186/s13287-018-1007-x

Figure legends.

Figure 1: De-adhesion dynamics of individual WJ-MSCs on treatment with EDTA was compared between control and serum-deprivation condition. Effect of serum deprivation stress on time constants of retraction was recorded with the help of time lapse imaging. The normalized area-vs.-time data were fitted to a Boltzmann sigmoid equation to determine the time constants τ1 and τ2 (A). Delayed de-adhesion under serum deprivation led to significant differences in τ1 and τ2 between serum-deprived and control WJ-MSCs (B). Comparison of wound induced migration between control and serum-deprived WJ-MSCs. Confluent monolayer cultures of control and serum-deprived WJ-MSCs were scratched with a sterile pipette tip at 0 h. Representative images of migration post scratch assay were obtained at 10 h, Scale bar: 500 um (C). Wound closure rate was also quantified. Each bar represents mean ± SEM (n = 5) (D). Representative DIC still images were captured from the time-lapse videos of control and serum-deprived WJ-MSCs. Black arrows identify the migration of some randomly selected cells. Numbers on the images indicate time in minutes and results are representative of three independent biological samples (n = 3) (E). To further investigate in detail the impact of serum deprivation on migration of WJ-MSCs, migration speed (F), trajectories of cells (G), directionality ratio (I) and MSD of cell body (H) were calculated and compared between control and serum-deprived WJ-MSCs for n = 150 cells from three different biological samples. Serum-deprived condition is denoted as no serum (NS) in the figure. Each bar represents mean ± SEM. (*P< 0.05, ***P< 0.001).

Figure 2. Effect of ERK pathway inhibition on VTN and MMP1 expression in serum-deprived WJ-MSCs. The mRNA and protein expression levels of MMP1 and VTN were detected by qRT-PCR (A, B) and Western blotting (C, D), respectively, in WJ-MSCs treated without and with ERK pathway inhibitor for 48h under serum deprivation condition. Impact of NF-κβ pathway inhibition on expression of VTN and MMP1. WJ-MSCs were transfected with a NC siRNA or a p65-targeted esiRNA for 48 h under serum-deprived state. The reduction in p65 protein level on transfecting with p65-targeted esiRNA was confirmed by Western blotting (E). The mRNA and protein expression levels of VTN and MMP-1 were detected by qRT-PCR (F, G) and Western blotting (H, I), respectively. *GAPDH* was used as endogenous control in qRT-PCR as well as a loading control in Western blotting. Band densities of Western blotting were quantified relative to GAPDH. Data shown are representative of at least three independent biological samples. Serum-deprived condition is denoted as no serum (NS) in the figure. Each bar represents mean±SEM (*P< 0.05, **P< 0.001, ***P< 0.001).

Figure 3: Effect of ERK pathway inhibition on cell spread area, de-adhesion dynamics and migration of serum-deprived WJ-MSCs. WJ-MSCs were treated with FR180204 for 48 h under serum deprived condition. Representative phase contrast images showing morphology are displayed (n = 3) (A). Cell area was quantified and compared for 150 cells from 3 different biological samples (B). A representative Gaussian distribution plot from 50 cells is presented to compare cell area between control and serum-deprived WJ-MSCs without and with ERK inhibitor treatment. Serum-deprived condition is denoted as no serum (NS) in the figure. ***p < 0.001(C). De-adhesion dynamics of FR180204 treated WJ-MSCs under serum deprivation. With the help of time lapse imaging, cell shape

changes during de-adhesion was quantified and recorded. The normalized area-vs.-time data were fitted to a Boltzmann sigmoid equation to determine the time constants τ1 and τ2 (D). Comparison of scratch-induced migration between control and serum-deprived WJ-MSCs without and with FR180204. Confluent monolayer cultures of control and treated WJ-MSC were wounded with a sterile pipette tip at 0 h. Images of migration post scratch assay were obtained at 10 h. Scale bar: 500 µm. Representative images from three independent biological samples (n = 3) are exhibited (E). Wound closure rate was calculated and compared between control and treated WJ-MSCs. Bar represents mean ± SEM (n = 3) (F). Effect of NF-κβ pathway inhibition on cell spread area, de-adhesion dynamics and migration of serum-deprived WJ-MSCs. WJ-MSCs were transfected with NC siRNA or p65-targeted esiRNA under serum-deprived condition. Representative phase contrast images showing morphology are displayed (n = 3) (G) Cell area was calculated for WJ-MSCs transfected with p65-targeted esiRNA or NC siRNA under serum starvation and plotted against control WJ-MSC samples. A sample size of 150 total cells, from three different biological samples, was used (H) A representative Gaussian distribution plot for 50 cells is presented to compare the cell area between control and transfected WJ-MSCs under serum deprivation (I). De-adhesion dynamics of p65 esiRNA transfected WJ-MSCs under serum deprivation. The change in cell area across time was quantified and fitted in Boltzmann sigmoid equation to determine the time constants. Differences in τ1 and τ2 between negative control siRNA and p65 esiRNA treated cells were plotted (J). Comparison of scratch wound- induced migration between control WJ-MSCs and WJ-MSCs transfected with NC siRNA or p65-targeted esiRNA under serum starvation was assessed. Representative images are shown (n = 4). Wound closure rate in µm/h was determined from scratch induced wound healing assay (K). Each bar represents mean ± SEM. (**P*< 0.05, ***P*< 0.001, ****P*< 0.001).

Figure 4: Effect of VTN knockdown on morphology, adhesion and migration of WJ-MSCs. Knockdown of VTN in WJ-MSCs, following transfection with VTN esiRNA, was validated by qRT-PCR. GAPDH was used as house-keeping gene (n=3) (A). Cell morphology images of WJ-MSCs transfected with VTN esiRNA or NC siRNA under serum starved condition for 48 hours in comparison to control condition are displayed. Scale bar: 500 µm. Cell spread area was compared between control WJ-MSCs and WJ-MSCs transfected with VTN esiRNA or NC siRNA under serum starved condition. A total of 150 cells from three different biological samples were used (B). A representative Gaussian distribution plot from 50 cells is shown (C). Effect of VTN knockdown on de-adhesion dynamics of serum-starved WJ-MSCs was quantified in terms of time taken for cellular detachment following EDTA treatment. The normalized change in cell spread area vs time was fitted to Boltzmann sigmoidal equation to obtain the time constants, t1 and t2. Significant reversal in the time constant values, τ1 and τ2 with knockdown of VTN under serum starved condition was observed. A total of 45 cells from 3 different biological samples were used for the assay (D). To compare the changes in actin cytoskeleton profile between control WJ-MSCs and WJ-MSCs transfected with VTN esiRNA or NC siRNA, actin stress fibres were visualized via immunofluorescence using Alexa Fluor 488-phalloidin (green) while DAPI (blue) was used to stain nuclei. Reduction in actin stress fibre formation upon VTN knockdown under serum starved condition is demonstrated in the representative immunofluorescence images (40X magnification) (n=3). Scale: 50 µm. Mean intensity of phalloidin staining was quantified and plotted (E). Impact of VTN knockdown on migration of serum-starved WJ-MSCs. Representative DIC images from different time intervals are marked with small black arrows to highlight migration of randomly selected cells from time-lapse imaging (F). Comparison of migration rate of control vs WJ-MSCs transfected with VTN esiRNA or NC siRNA under serum starved condition is shown by the bar graph for 150 cells from three independent biological samples (H). For further insight, cell trajectory pattern (G), directionality ratio(I) and mean square displacement(J) were quantified from the analysis of DIC time lapse imaging videos for 150 cells from three independent biological sample . mRNA expression levels of ECM genes like *MMP-1, COL1A1, COL11A1 and COL12A1* was quantified following VTN knockdown under serum starved condition using qRT-PCR (n=3)(K). Serum-deprived condition is denoted as no serum (NS) in the figure. Each bar represents mean ± SEM. (**P*< 0.05, ***P*< 0.001, ****P*< 0.001).

Figure 5: Effect of hypoxia on morphology, adhesion and migration of WJ-MSCs and its co-relation with VTN expression. Cell morphology and cell spread area were compared between WJ-MSCs cultured under control and hypoxia (2% O_2) conditions. Scale: 500 µm (A, B). A representative Gaussian distribution plot reflecting cell spread area comparison for 50 cells is shown (n=3) (C). Cellular de-adhesion dynamics under hypoxia was studied via time lapse imaging of hypoxic WJ-MSCs following EDTA treatment. The normalized cell area vs time data was fitted in Boltzmann sigmoidal equation to obtain the $\tau 1$ and $\tau 2$ time constant values for a total of 45 cells from three independent biological samples (D). To analyse the cellular migration of WJ-MSCs under hypoxia condition, migration rate (E), cell trajectories (F) and directionality ratio (G) were quantified from DIC time lapse imaging of a total of 60 cells from two independent biological samples. mRNA (H) and protein expression levels (I) of MMP-1 and VTN were examined under hypoxia condition and compared against control condition from three independent biological samples. GAPDH was considered as an internal control for both mRNA and protein quantifications (n=3). Actin cytoskeleton profile of control and hypoxia treated WJ-MSCs were visualized via immunofluorescence using Alexa Fluor 488-phalloidin (green) while DAPI (blue) was used to stain nuclei. Representative immunofluorescence images (at 40X magnification) and immunofluorescence mean intensity quantification plot demonstrated no significant change in actin cytoskeleton profile (n=3) (J). Effect of ERK pathway inhibition with FR180204 on WJ-MSCs under hypoxia condition. WJ-MSCs were treated with FR180204 for 48 hours under hypoxia condition. The mRNA and protein expression of VTN was quantified by qRT-PCR and Western blotting respectively (K, L), in WJ-MSCs treated with or without ERK inhibitor, FR180204. The change in cellular morphology was quantified in terms of cell spread area and plotted from 150 cells obtained from 3 independent biological samples (M). De-adhesion dynamics of WJ-MSCs under hypoxia condition, with or without ERK inhibitor, FR180204 was studied via time lapse imaging. The normalized cell area was fitted in Boltzmann sigmoidal equation and the time constants $\tau 1$ and $\tau 2$ were plotted for a total of 30 cells from 2 independent biological samples (N). Each bar represents mean ± SEM. (*$P < 0.05$, **$P < 0.001$, ***$P < 0.001$).

Fig 1

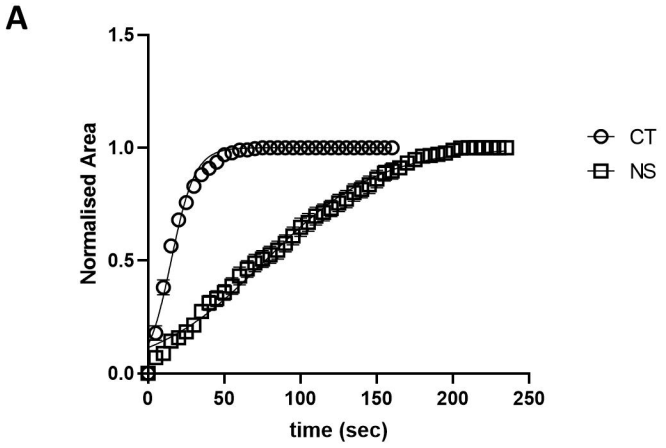
A
Normalised Area
time (sec)
CT
NS

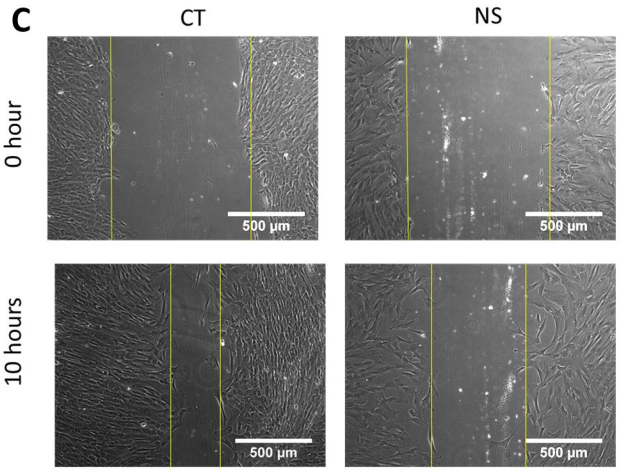
C
CT
NS
0 hour
10 hours
500 µm

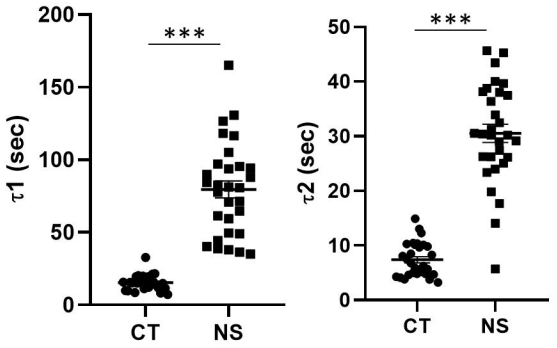
B
τ1 (sec)
τ2 (sec)
***
CT
NS

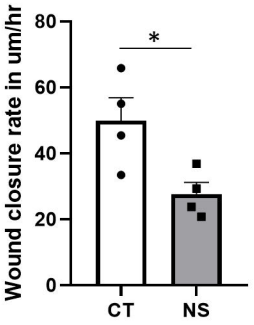
D
Wound closure rate in um/hr
*
CT
NS

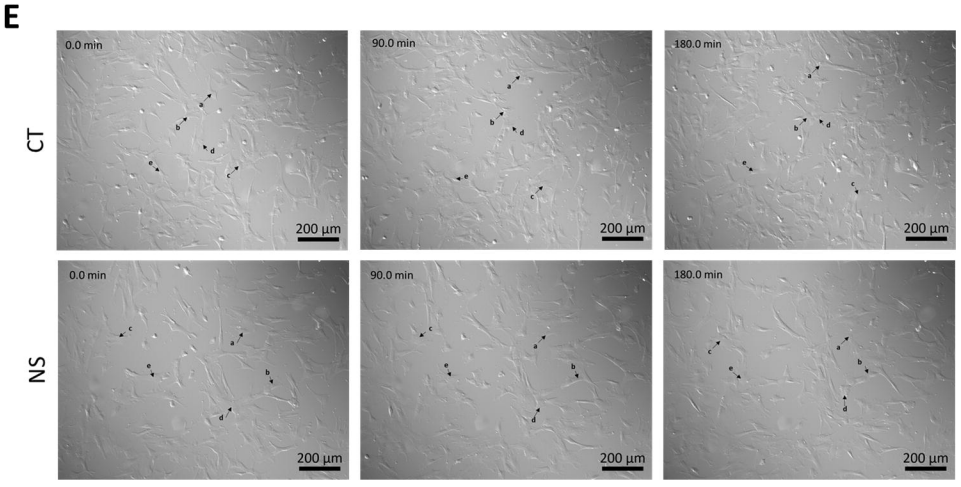
E
CT
NS
0.0 min
90.0 min
180.0 min
200 µm

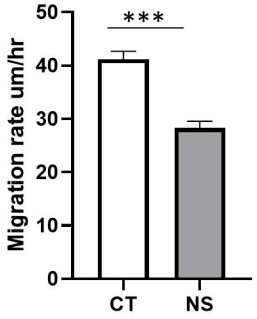
F
Migration rate um/hr
***
CT
NS

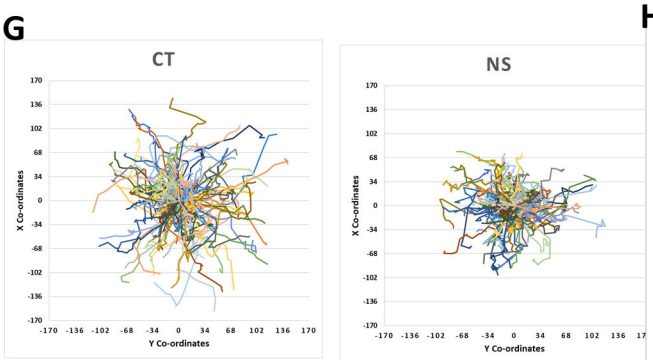
G
CT
NS
X Co-ordinates
Y Co-ordinates

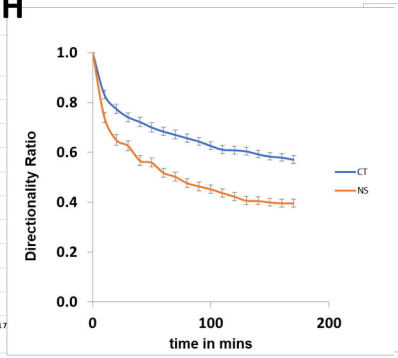
H
Directionality Ratio
time in mins
CT
NS

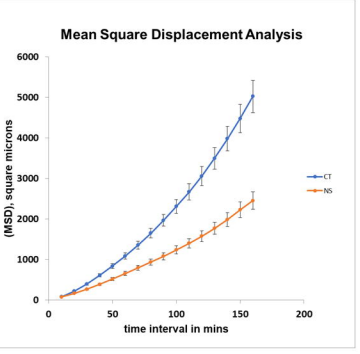
I
Mean Square Displacement Analysis
(MSD), square microns
time interval in mins
CT
NS

Fig 2

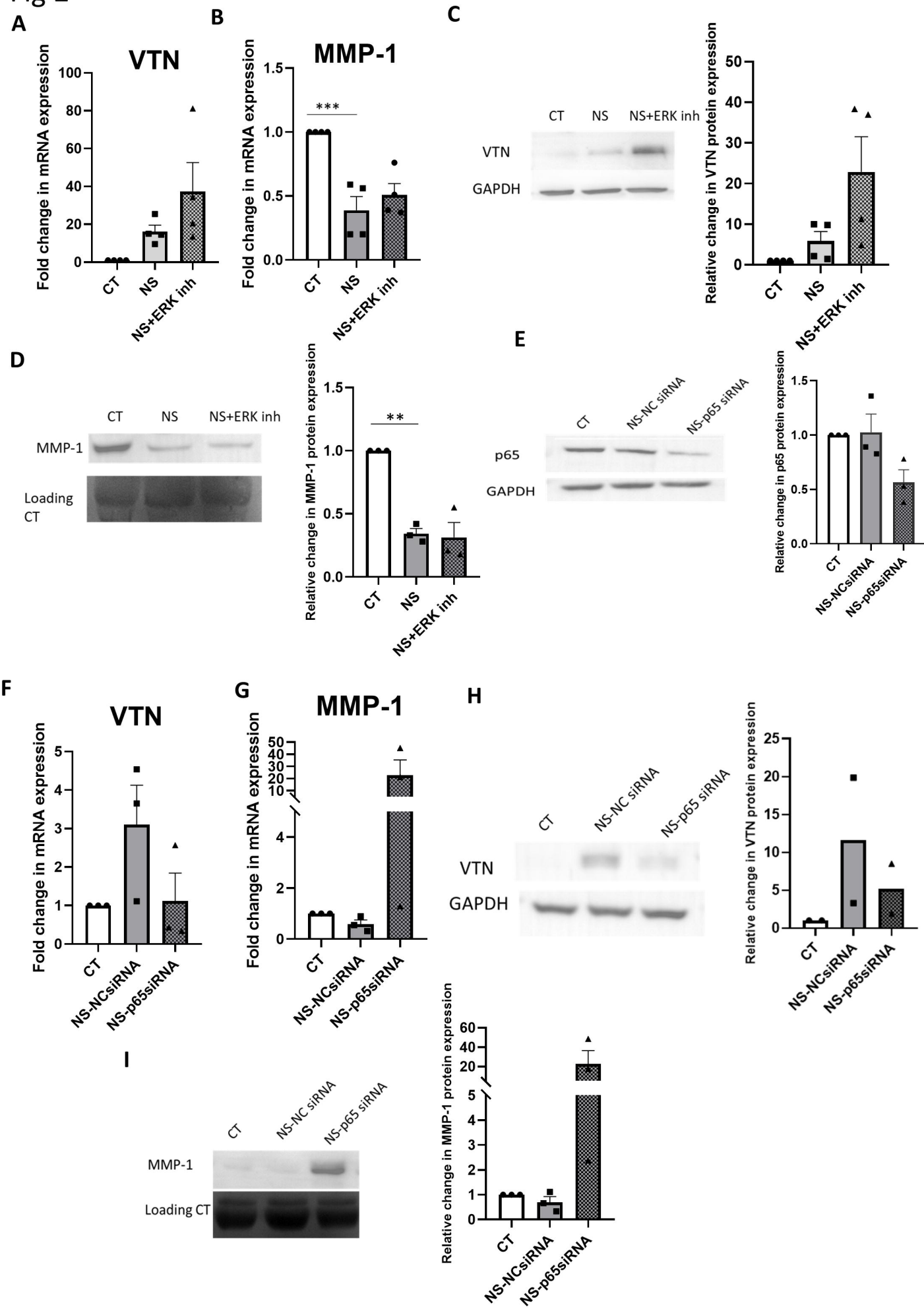
A
VTN
Fold change in mRNA expression
100
80
60
40
20
0
CT
NS
NS+ERK inh
B
MMP-1
Fold change in mRNA expression
1.5
1.0
0.5
0.0
***
CT
NS
NS+ERK inh
C
CT
NS
NS+ERK inh
VTN
GAPDH
Relative change in VTN protein expression
50
40
30
20
10
0
CT
NS
NS+ERK inh
D
CT
NS
NS+ERK inh
MMP-1
Loading CT
Relative change in MMP-1 protein expression
1.5
1.0
0.5
0.0
**
CT
NS
NS+ERK inh
E
CT
NS-NC siRNA
NS-p65 siRNA
p65
GAPDH
Relative change in p65 protein expression
1.5
1.0
0.5
0.0
CT
NS-NCsiRNA
NS-p65siRNA
F
VTN
Fold change in mRNA expression
5
4
3
2
1
0
CT
NS-NCsiRNA
NS-p65siRNA
G
MMP-1
Fold change in mRNA expression
50
40
30
20
10
4
2
0
CT
NS-NCsiRNA
NS-p65siRNA
H
CT
NS-NC siRNA
NS-p65 siRNA
VTN
GAPDH
Relative change in VTN protein expression
25
20
15
10
5
0
CT
NS-NCsiRNA
NS-p65siRNA
I
CT
NS-NC siRNA
NS-p65 siRNA
MMP-1
Loading CT
Relative change in MMP-1 protein expression
60
40
20
5
4
3
2
1
0
CT
NS-NCsiRNA
NS-p65siRNA

Fig 3

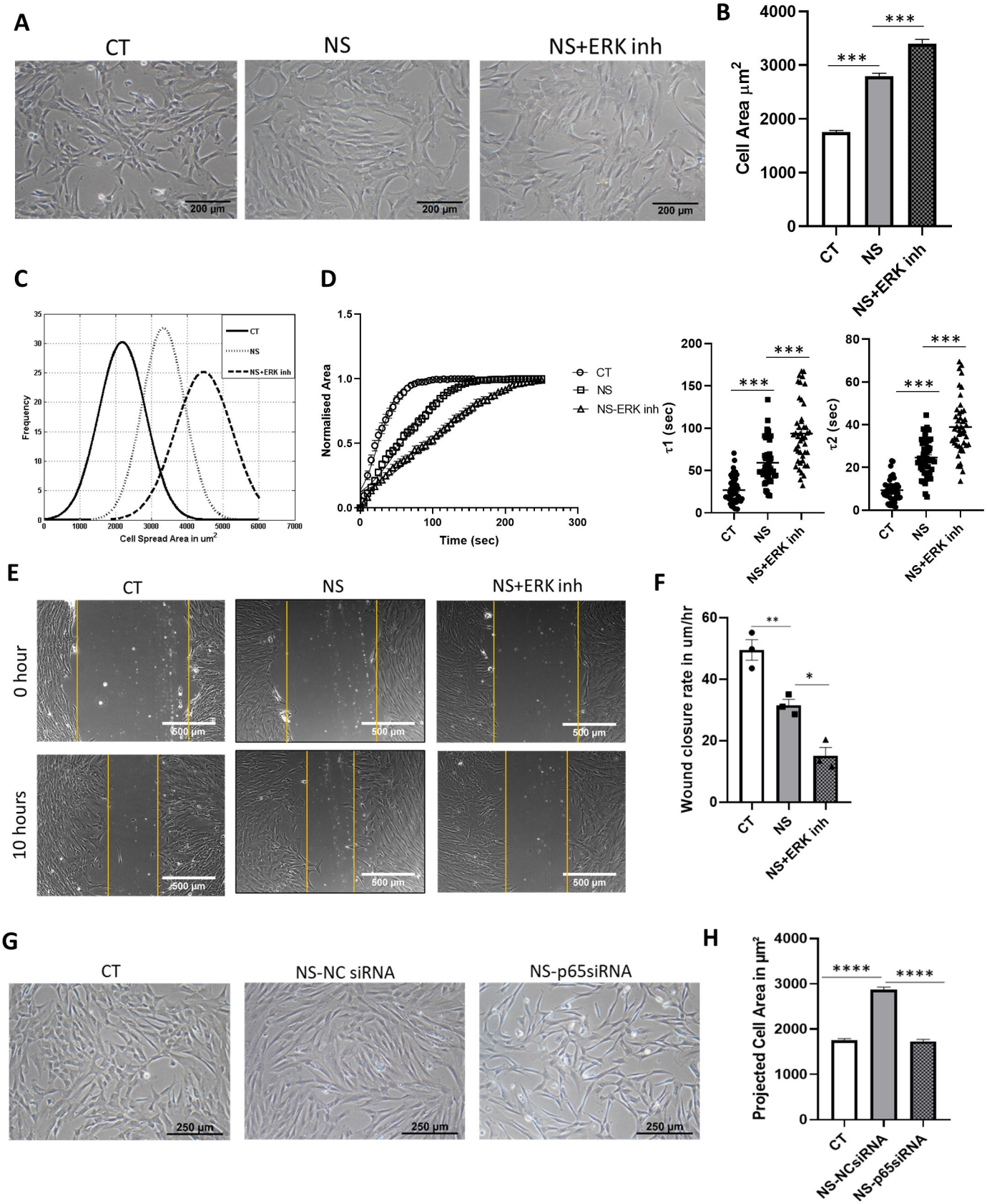
A
CT
NS
NS+ERK inh
200 µm
B
Cell Area µm²
***
***
CT
NS
NS+ERK inh
C
Frequency
Cell Spread Area in um²
CT
NS
NS+ERK inh
D
Normalised Area
Time (sec)
CT
NS
NS-ERK inh
τ1 (sec)
τ2 (sec)
E
CT
NS
NS+ERK inh
0 hour
10 hours
500 µm
F
Wound closure rate in um/hr
**
*
G
CT
NS-NC siRNA
NS-p65siRNA
250 µm
H
Projected Cell Area in µm²
****
****
CT
NS-NCsiRNA
NS-p65siRNA

Fig 3 cont.

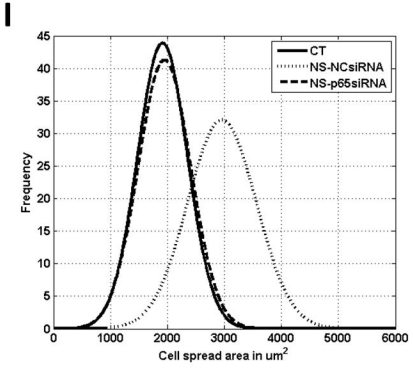
I
CT
NS-NCsiRNA
NS-p65siRNA
Frequency
Cell spread area in um2

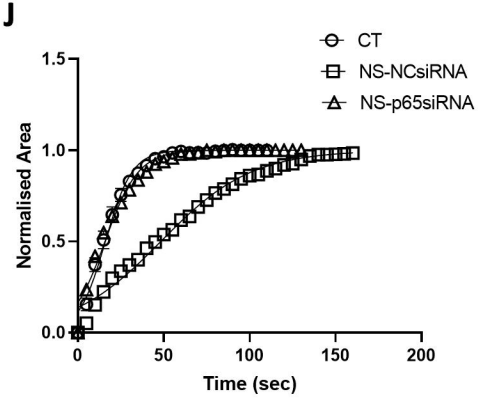
J
CT
NS-NCsiRNA
NS-p65siRNA
Normalised Area
Time (sec)

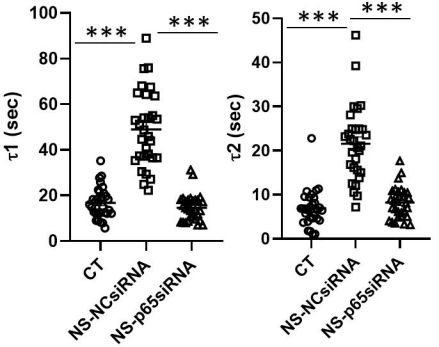
τ1 (sec)
τ2 (sec)
***
CT
NS-NCsiRNA
NS-p65siRNA

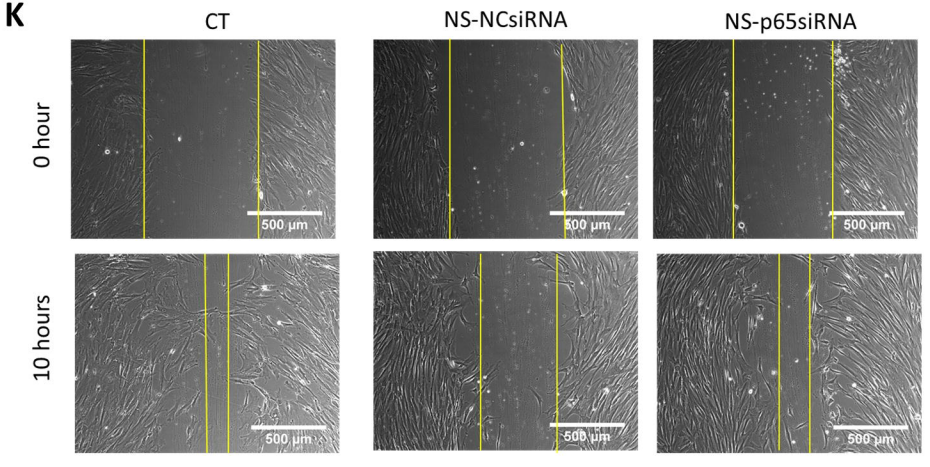
K
CT
NS-NCsiRNA
NS-p65siRNA
0 hour
10 hours
500 µm

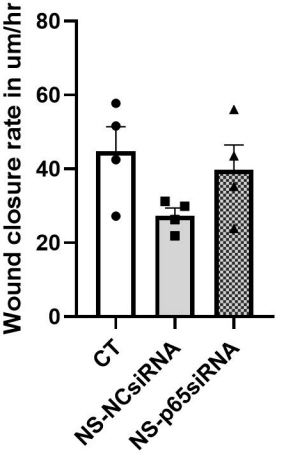
Wound closure rate in um/hr
CT
NS-NCsiRNA
NS-p65siRNA

Fig 4

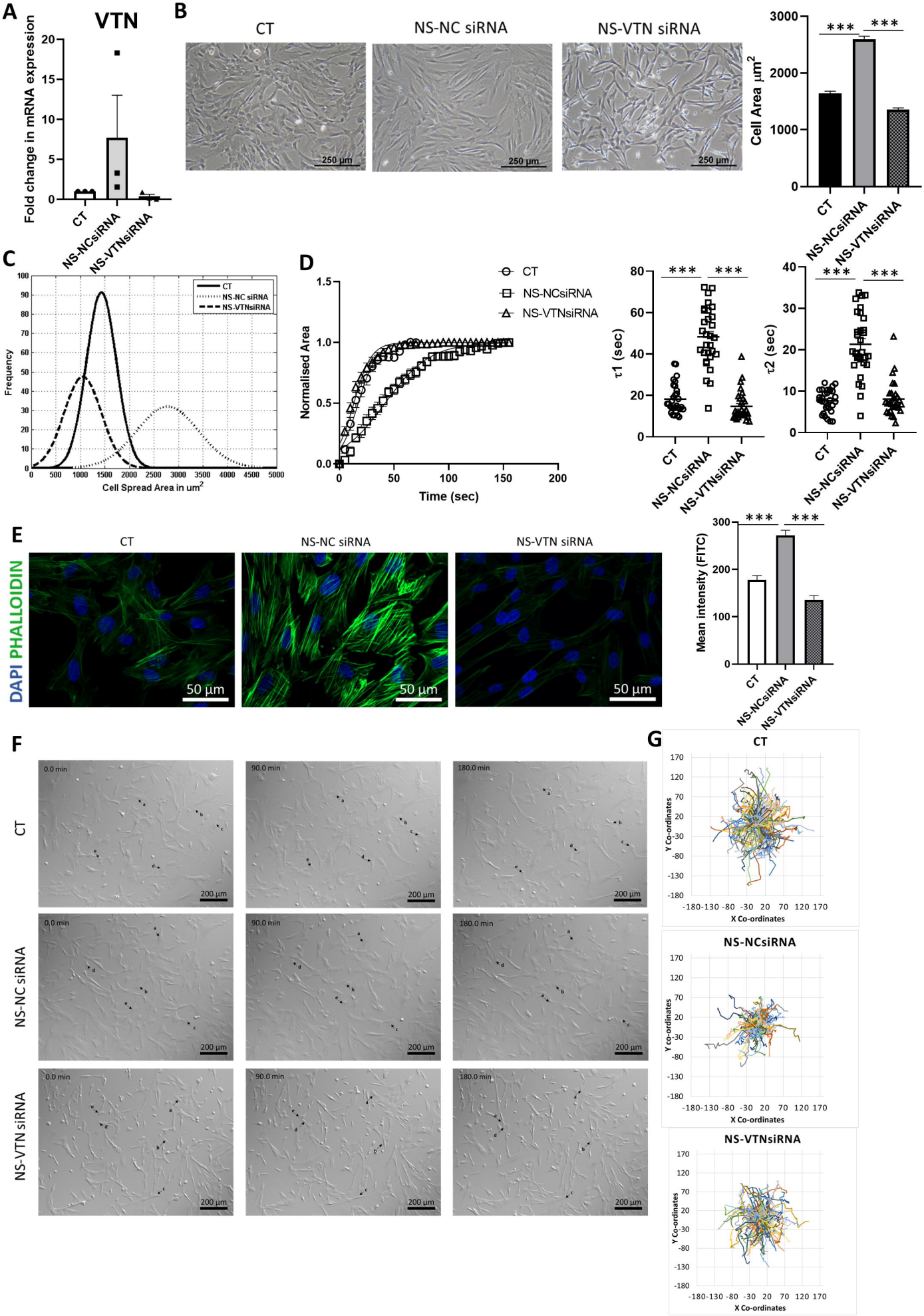
A
VTN
Fold change in mRNA expression
CT
NS-NCsiRNA
NS-VTNsiRNA
B
CT
NS-NC siRNA
NS-VTN siRNA
250 µm
Cell Area µm²
***
C
Frequency
Cell Spread Area in um²
D
Normalised Area
Time (sec)
τ1 (sec)
τ2 (sec)
E
DAPI PHALLOIDIN
50 µm
Mean intensity (FITC)
F
0.0 min
90.0 min
180.0 min
200 µm
G
Y Co-ordinates
X Co-ordinates

Fig 4 cont.

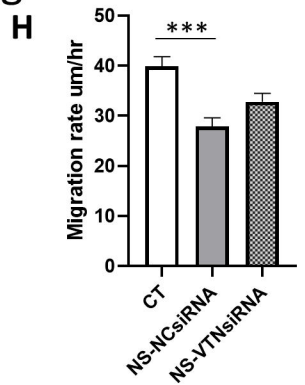
H
***
Migration rate um/hr
50
40
30
20
10
0
CT
NS-NCsiRNA
NS-VTNsiRNA

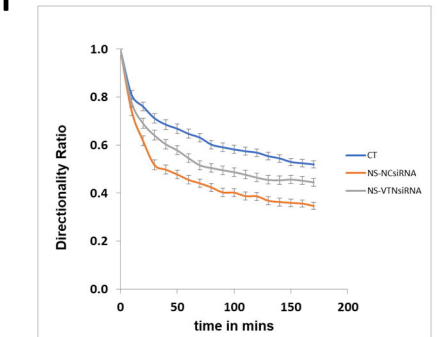
I
Directionality Ratio
1.0
0.8
0.6
0.4
0.2
0.0
0
50
100
150
200
time in mins
CT
NS-NCsiRNA
NS-VTNsiRNA

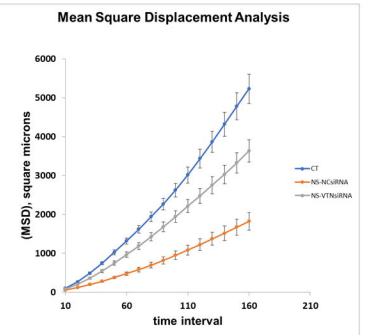
J
Mean Square Displacement Analysis
(MSD), square microns
6000
5000
4000
3000
2000
1000
0
10
60
110
160
210
time interval
CT
NS-NCsiRNA
NS-VTNsiRNA

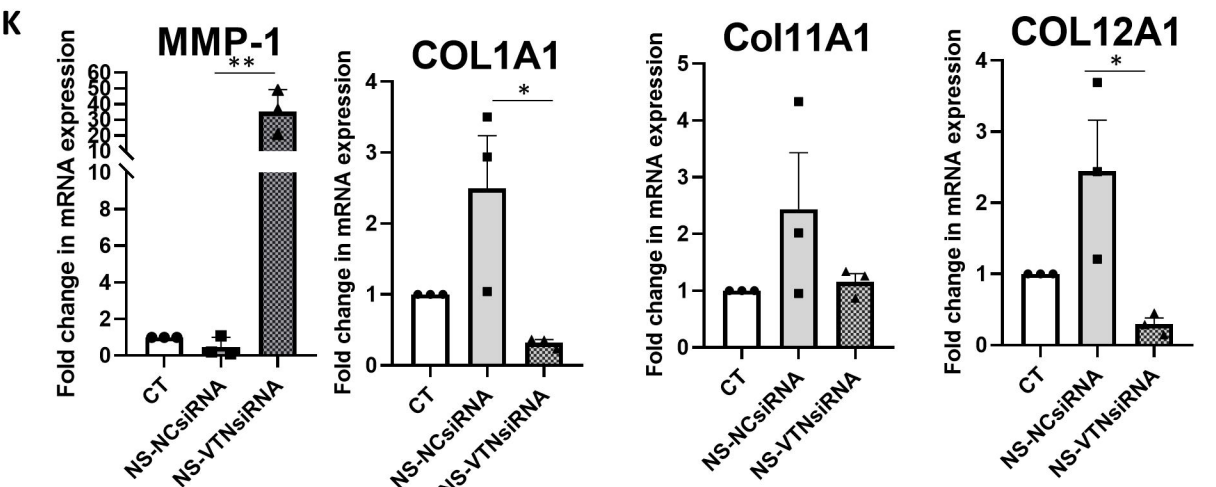
K
MMP-1
**
Fold change in mRNA expression
60
50
40
30
20
10
10
8
6
4
2
0
CT
NS-NCsiRNA
NS-VTNsiRNA
COL1A1
*
Fold change in mRNA expression
4
3
2
1
0
CT
NS-NCsiRNA
NS-VTNsiRNA
Col11A1
Fold change in mRNA expression
5
4
3
2
1
0
CT
NS-NCsiRNA
NS-VTNsiRNA
COL12A1
*
Fold change in mRNA expression
4
3
2
1
0
CT
NS-NCsiRNA
NS-VTNsiRNA

Fig 5

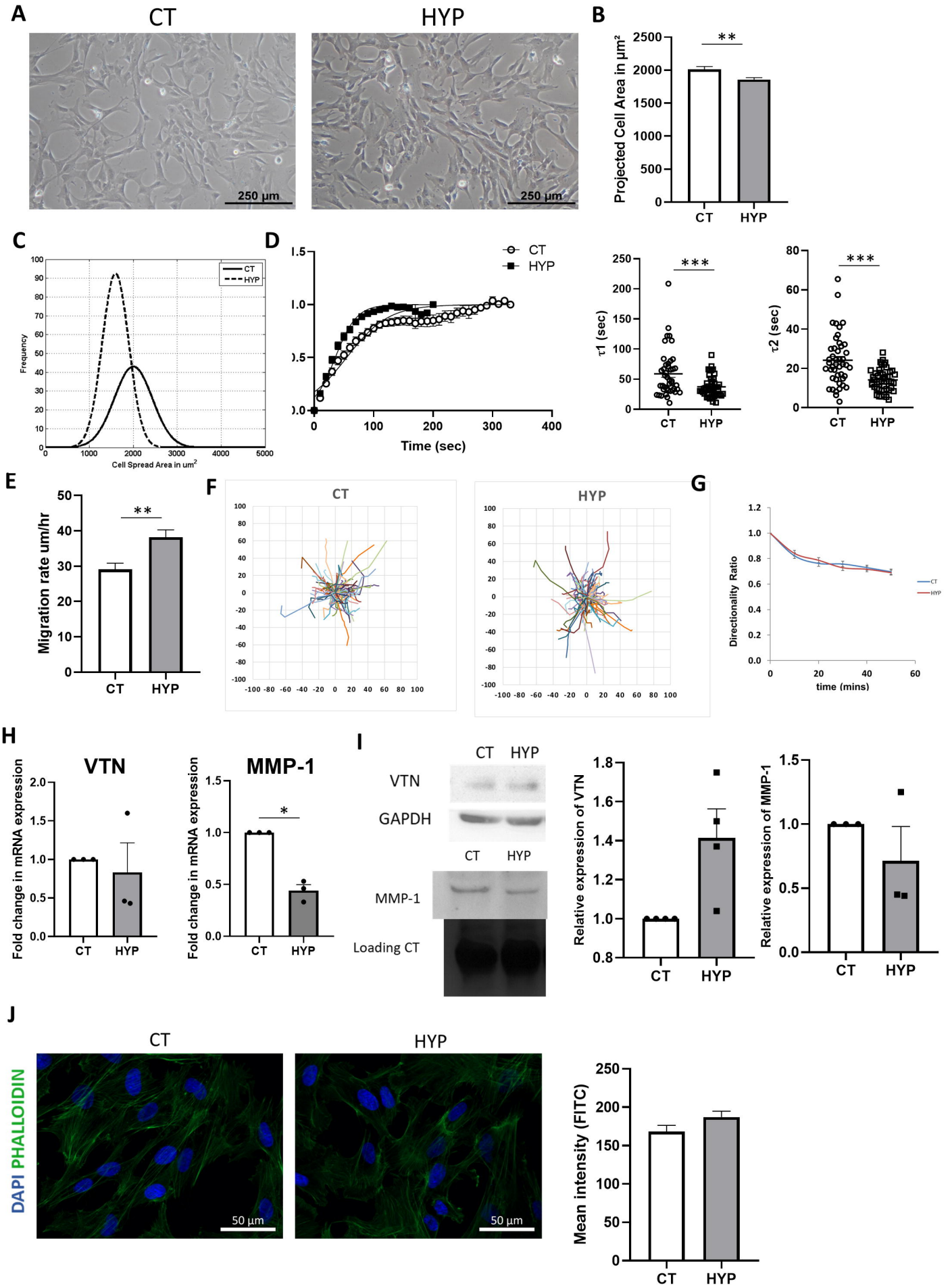
A
CT
HYP
250 µm
250 µm
B
Projected Cell Area in µm²
**
CT
HYP
C
Frequency
Cell Spread Area in um²
CT
HYP
D
CT
HYP
Time (sec)
τ1 (sec)
***
τ2 (sec)
***
E
Migration rate um/hr
**
F
CT
HYP
G
Directionality Ratio
time (mins)
H
VTN
MMP-1
Fold change in mRNA expression
*
I
CT HYP
VTN
GAPDH
MMP-1
Loading CT
Relative expression of VTN
Relative expression of MMP-1
J
CT
HYP
DAPI PHALLOIDIN
50 µm
50 µm
Mean intensity (FITC)

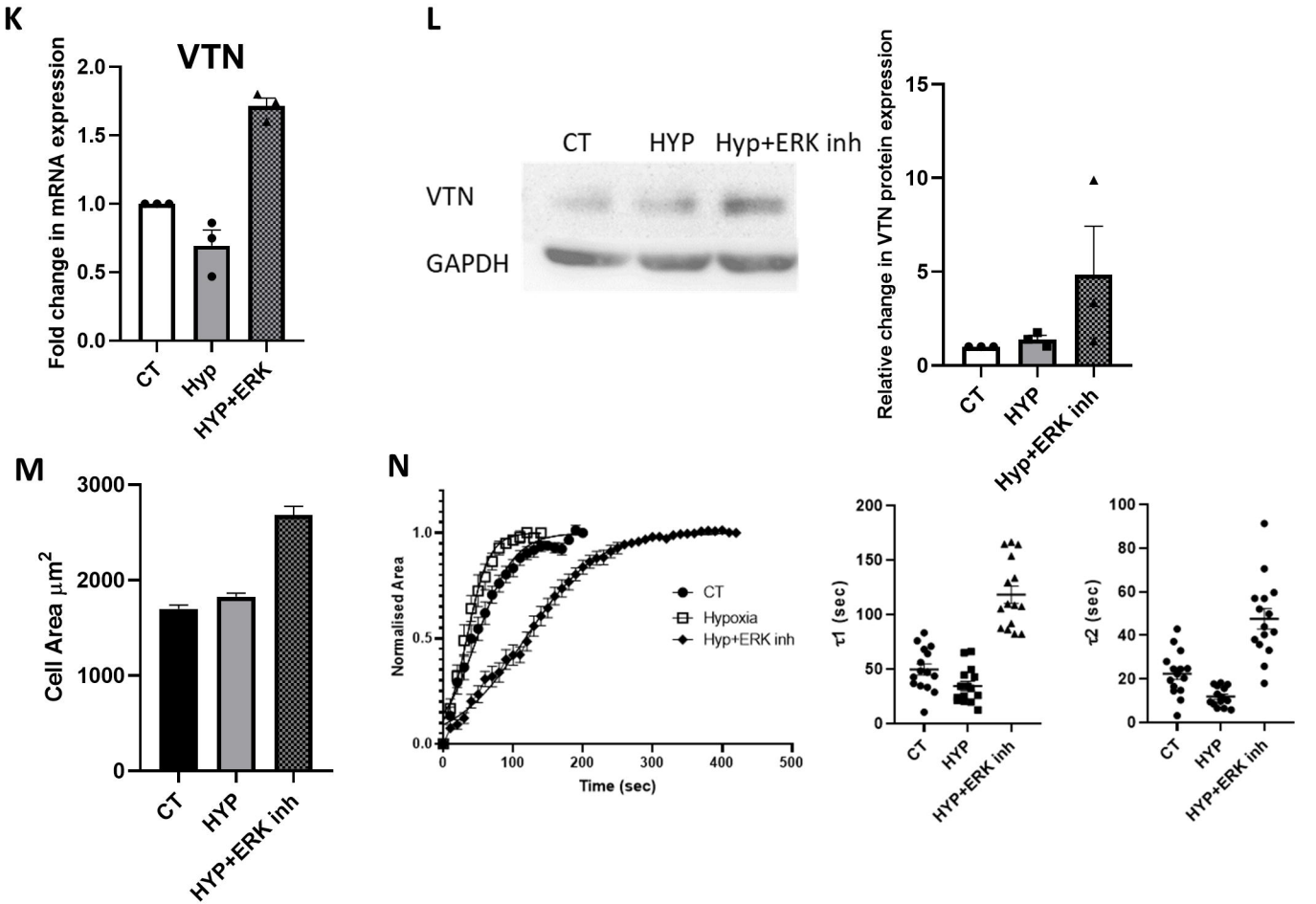
K
VTN
Fold change in mRNA expression
2.0
1.5
1.0
0.5
0.0
CT
Hyp
HYP+ERK
L
CT
HYP
Hyp+ERK inh
VTN
GAPDH
Relative change in VTN protein expression
15
10
5
0
CT
HYP
Hyp+ERK inh
M
Cell Area μm2
3000
2000
1000
0
CT
HYP
HYP+ERK inh
N
Normalised Area
1.0
0.5
0.0
0
100
200
300
400
500
Time (sec)
CT
Hypoxia
Hyp+ERK inh
τ1 (sec)
200
150
100
50
0
CT
HYP
HYP+ERK inh
τ2 (sec)
100
80
60
40
20
0
CT
HYP
HYP+ERK inh